Int J Clin Exp Med 2018;11(12):12991-13002
www.ijcem.com /ISSN:1940-5901/IJCEM0086403

Original Article

Identification of colorectal cell exosomes by Raman spectral analysis

Weiwei Zheng[1], Wei Huang[1], Jianxin Chen[1], Jiqiu Zhou[1], Xiong Xu[1], Gang Xu[1], Ruiyuan Chen[1], Guiwen Wang[2], Sen Zhang[1]

[1]*Department of Colorectal and Anal Surgery, The First Affiliated Hospital of Guangxi Medical University, Nanning 530021, Guangxi, P.R. China;* [2]*Guangxi Academy of Sciences, Nanning 530007, Guangxi, P.R. China*

Received October 7, 2018; Accepted November 8, 2018; Epub December 15, 2018; Published December 30, 2018

Abstract: Purpose: The goal of this study was to determine the marker spectra of purified colorectal cancer (CRC) exosomes by Raman spectra analysis. Methods: Culture supernatants of different malignant CRC tumor and immune cells were collected and centrifuged to obtain exosome samples. The facticity and purity of the exosomes were identified by electron microscopy. Flow cytometry (FCM) analysis was used to determine their size and composition. Nanoparticle Tracking Analysis (NTA) was adopted to identify surface specific marker proteins. The non-invasive, label-free Raman spectroscopy technique was used to detect large numbers of identified exosomes. Results: A standard spectrum for CRC diagnosis was constructed through analysis of tumor exosome spectra. Overall expression levels of exosome surface proteins were found to be increased and most of the surface protein levels were increased compared with those from normal benign cells ($p<0.05$). There were many similar peaks in exosomes of colorectal cancer, indicating that they contain same substances and abundances in crucial proteins and nucleic acids, which have the potential to become biomarkers. Conclusion: This novel method is non-invasive and can be used in clinical diagnosis to observe tiny biomolecular structures *in situ* which is suitable for biomarker discovery studies.

Keywords: Exosomes, colorectal cancer, Raman spectroscopy, surface protein, marker spectrum, nanoparticle tracking analysis

Introduction

Malignant tumors of the digestive system, especially colorectal cancer (CRC), have been increasing {Cai, 2015 #1; Belov, 2016 #113}. CRC is one of the most common malignancies in the United States and accounts for approximately 10% of global cancer incidence [1]. However, symptoms of early-stage cancers are minor and not easily detected. The differences between normal cells and rudimentary cancer cells are too slight to be detected by common morphological methods [2]. Thus, colorectal cancer diagnosis requires more sensitive molecular markers.

Exosomes are nanosized [3] vesicles ranging in size from 40 to 200 nm (1.13-1.18 g/ml density) that are present in a cell's surrounding fluids. Exosomes are generated inside the cytoplasm, and their cargo, therefore, represents a molecular biology fingerprint of the cell of origin and is useful for identifying cellular phenotypes and genotypes [4]. Recent studies have shown that exosomes actually contain functional biological material and represent a vital subset of microvesicular communication in the body. Exosomes also play an important role in cancer metastasis through the regulation of tumorigenic pathways [5]. Therefore, they have been thought of as a cancer biomarker. However, there are only two efficient methods to extract and purify exosomes: (1) differential/gradient ultracentrifugation [6] and (2) low-speed centrifugation with commercial isolation kits [7]. Extensive practices show that differential ultracentrifugation methods [8], which separate exosomes by size and/or buoyant density, lead to higher purity of the desired vesicle population, but they remain quite time-consuming and are not appropriate for applications [9].

Thus, simpler and faster methods, such as laser optical tweezers with Raman spectrosco-

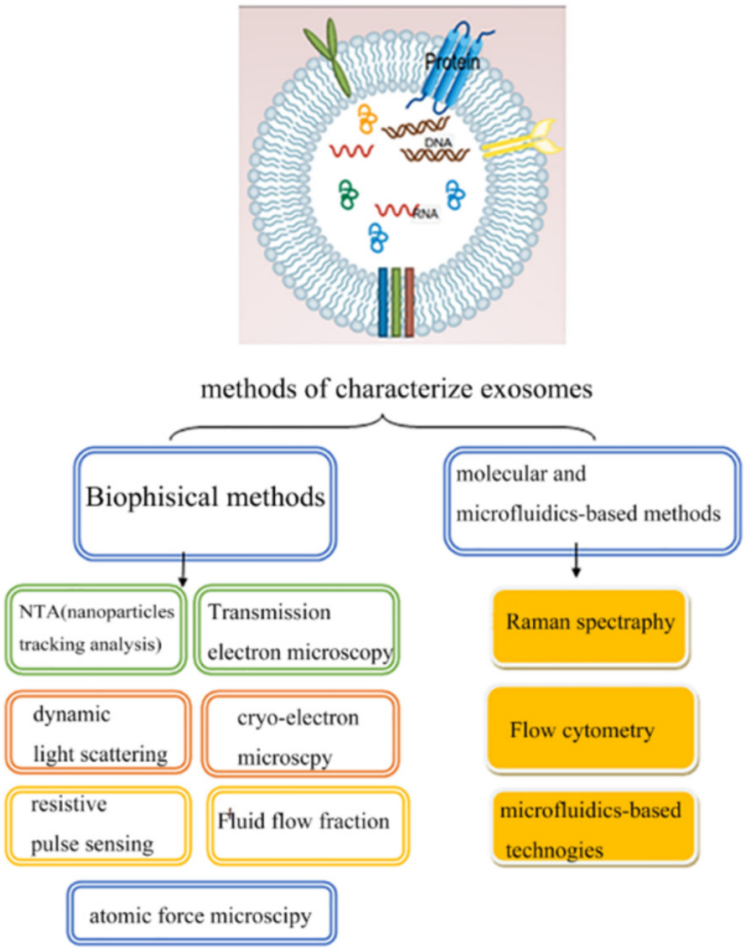

Figure 1. Overview of exosome characterization methodologies, including biophysical methods, and molecular and microfluidics-based methods. Biophysical methods include NTA, TEM, DLS, Cryo-M, RPS, FFF and AFM. But according to the identification performance of these methods, our group chose NTA and TEM as the identification methods. In addition, molecular and microfluidics-based methods include Raman spectroscopy, Flow cytometry, and microfluidics-based technologies. Also based on the characteristics of these methods, our group chose Raman spectroscopy and Flow cytometry.

py, are investigated to analyze the molecular components of exosomes. Raman spectroscopy, a vibrational analysis technique, is gaining popularity in cancer diagnosis. Raman spectroscopy can support gold-standard techniques and substantially improve clinical diagnosis [10]. Although other optical methods have also been used to analyze exosomes, many of them offer only limited biochemical information [11]. For example, fluorophore-assisted methods provide biochemical information for only targeted biological components in the exosome, and other scattering techniques (nanoparticle tracking analysis, NTA) [11] merely provide physical information, such as the size distribution of the exosomes (**Figure 1**).

To better characterize exosome content, we decided to employ specifically laser optical tweezers with Raman spectroscopy. This optical spectroscopy method could reveal the ratios between proteins, nucleic acids, and lipids and the changes in these ratios under different physiological conditions [12]. However, optical lasers only allow the measurement of single exosome, making the collection of sufficient data extremely laborious and slow. Additionally, this method lacks surface specificity. Moreover, most minute particles, especially exosomes, must remain in a liquid environment to maintain their normal biological function [4]. Brownian motion makes it difficult to locate a single exosome and collect its Raman spectra [13]. In the past, common chemical fixation or micropipetting techniques have been adopted, However, both approaches exert strong effects on the surrounding biological environment [14, 15].

The improvement of optical tweezers has gradually solved this problem. Raman tweezers are a kind of optical technology that combines laser optical tweezers with Raman spectroscopy to study single biological cell or organelle in a near-natural state [16]. These tweezers trap a tiny sample in suspension. The optical fixing technology does not involve any mechanical contact, does not cause cell surface effects, and does not require any chemical agent. Therefore, living cells can undergo long-term Raman spectroscopy probing [17]. The technology not only overcomes the defects of the fixed technique in traditional Raman spectroscopy detection but also improves the activity of biological mononuclear cells. Also this technique

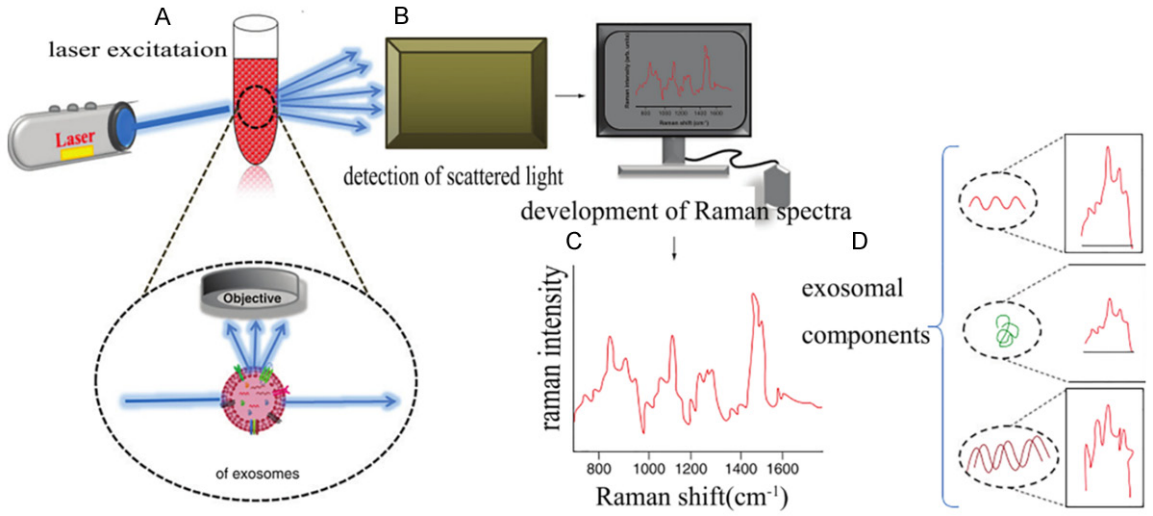

Figure 2. Raman spectroscopy flow chart. A laser is focused to trap exosomes mounted on a high-purity quartz glass groove in fluid (e.g. PBS) (A). Molecular vibration spectra of individual exosomes are captured (B) and processed to obtain the Raman spectrogram, including individual constituents (C & D). PBS: phosphate-buffered saline.

affords real-time tracking of biochemical kinetic processes, which can help us gain a deeper understanding of the behavior of macromolecules in the cell [18] (**Figure 2**).

In this study, methods of identifying exosome characteristics were comprehensively assessed [19]. Raman spectra was found to be a fast, non-invasive method for easy examination and extraction of materials. After the standard spectrum of a certain type of cancer is screened out, the spectral curve of the patient's blood could be used to confirm the diagnosis.

Materials and methods

Cell culture

Exosome-depleted FBS Media Supplement (EXO-FBS-250A-1) was provided by Genetimes ExCell Technology, Inc, affiliated to System Biosciences (SBI). The CT-26.WT and Mc38 cell lines (mouse colon cancer cells, purchased in Zhongqiao Xinzhou Company, Shanghai) were cultured in RPMI 1640 medium (Gibco, Grand Island, New York.US) with 10% FBS and 1% penicillin/streptomycin (Gibco, Grand Island, New York.US). Ana-1 cells (Chinese Academy of Sciences Shanghai Cell Bank, Shanghai) were cultured in RPMI 1640 medium with 10% FBS and 1% penicillin/streptomycin. All cell lines were cultured at 37.5°C in 5% CO_2. This study has been approved by the Ethics Committee of the First Affiliated Hospital of Guangxi Medical University.

Exosome isolation and purification

A total of 240 ml of cell culture medium was centrifuged with a 32Ti Rotator at 500× g for 15 min at 4°C to remove detached cells. The supernatants were centrifuged at 2000× g for 20 min at 4°C to remove cell debris and then at 16,000× g for 40 minutes at 4°C to remove additional cell debris and microvesicles. The supernatants were collected and filtered using a 0.22 μm filter from JET BIOFIL. These filtered supernatants were centrifuged at 120,000× g for 70 minutes at 4°C and were then thrown away, retaining the deposits. The deposits were resuspended in 40 ml of filtered phosphate-buffered saline (PBS). The resulting fluid was centrifuged again at 120,000× g for 70 minutes at 4°C, and the supernatants were thrown away. The sediments were considered exosomes and were diluted in 100 μl of phosphate-buffered saline (PBS). All centrifugation was performed at 4°C. The final solution containing exosomes was preserved at -80°C.

Transmission electron microscopy (TEM)

The solution was mixed with an equal volume of 4% paraformaldehyde (PFA). Then, 8 μl of the mixture was deposited on electron-microscope grids made of copper. After a series of standard

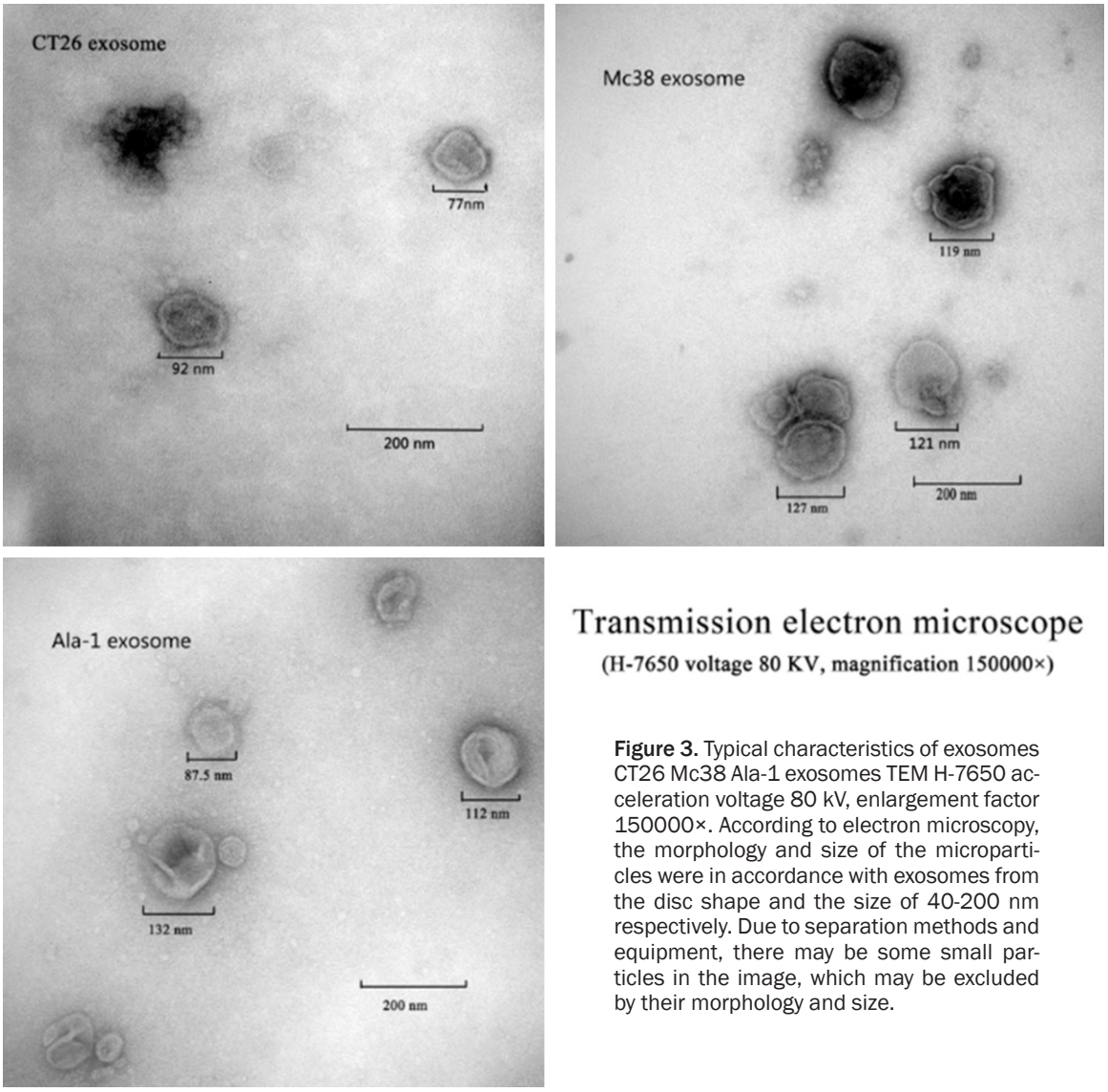

Figure 3. Typical characteristics of exosomes CT26 Mc38 Ala-1 exosomes TEM H-7650 acceleration voltage 80 kV, enlargement factor 150000×. According to electron microscopy, the morphology and size of the microparticles were in accordance with exosomes from the disc shape and the size of 40-200 nm respectively. Due to separation methods and equipment, there may be some small particles in the image, which may be excluded by their morphology and size.

treatments, the solution was volatilized, and the grids were observed by TEM at 200 kV.

Flow cytometry (FCM)

Samples of exosomes extracted from nutrient solution derived from CT26, MC38 and Ala-1 cells were sealed and preserved at -80°C. These samples were melted slowly at 4°C and then divided into twelve portions. CT26 exosomes sample was equally divided into 4 portions and added to 4 flow tubes and 2 μl of CD9-FITC was added to the first flow tube, 2 μl of CD63-APC to the second flow tube, and 2 μl of both CD9-FITC and CD63-APC to the third flow tube, then 2 μl of PBS was added to the fourth flow tube as a blank. Incubate at 37°C for 30 minutes after mixing gently. After the incubation, 2 ml of PBS buffer was added to each flow tube and centrifuged at 300-400 g for 5 minutes at 4°C, and discard the supernatant. After resuspending the cells in PBS buffer, a flow test was performed and the results were analyzed. The other 2 samples were also treated in same method.

Nanosight detection of exosome size

The dynamic light-scattering method was used to measure exosome particle size distribution. The collected exosomes were diluted with PBS to a particle concentration of 10^6/ml and injected into a Nanosight NS300 Nanoparticle Tracking Analyzer (NTA) with a 1 ml syringe.

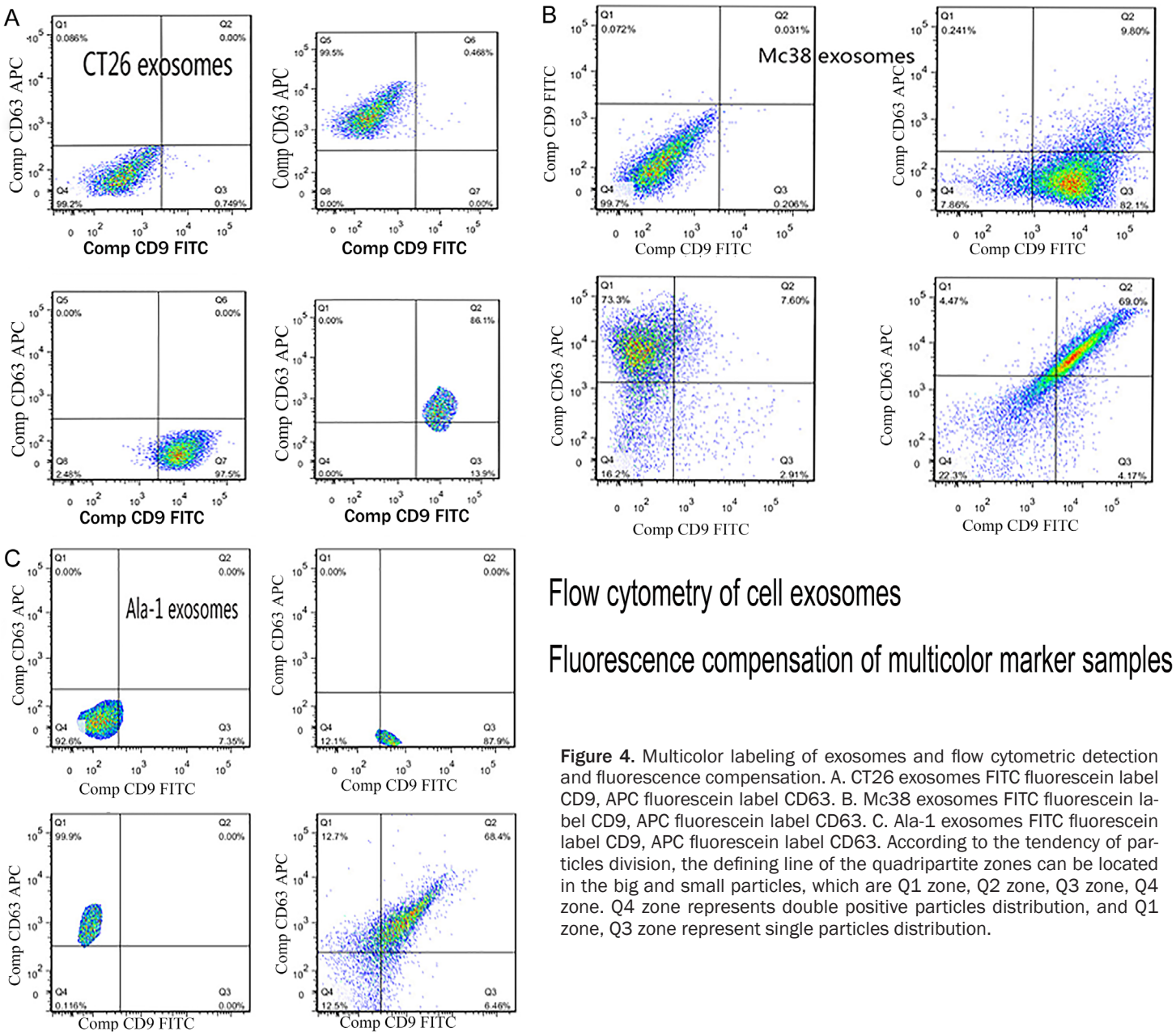

Figure 4. Multicolor labeling of exosomes and flow cytometric detection and fluorescence compensation. A. CT26 exosomes FITC fluorescein label CD9, APC fluorescein label CD63. B. Mc38 exosomes FITC fluorescein label CD9, APC fluorescein label CD63. C. Ala-1 exosomes FITC fluorescein label CD9, APC fluorescein label CD63. According to the tendency of particles division, the defining line of the quadripartite zones can be located in the big and small particles, which are Q1 zone, Q2 zone, Q3 zone, Q4 zone. Q4 zone represents double positive particles distribution, and Q1 zone, Q3 zone represent single particles distribution.

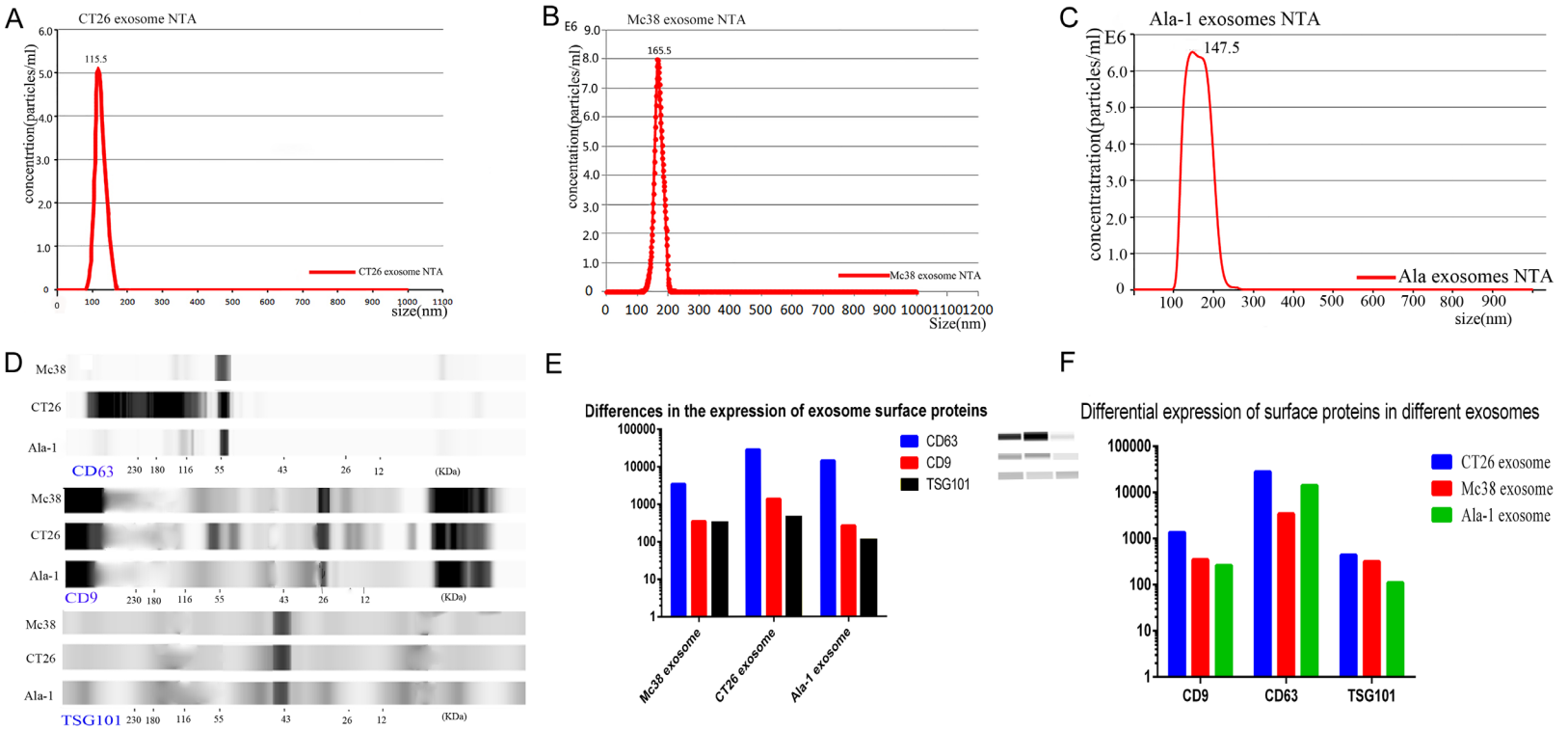

Figure 5. CT26, Mc38, or Ala-1 exosome NTA and exosome-specific marker proteins. First, the first three red line drawings show the particle size of different types of exosomes. The drawings revealed that the size of exosomes of CT26 mainly distributed in 60-160 nm (A), Mc38 exosomes distributed in 110-200 nm (B), Ala-1 exosomes distributed in 100-240 nm (C), the size of which are slightly larger than that of conventional exosomes. Second, WB detection of the three proteins on the surface of each exosome was based on the band (D). The expression of CD63 protein at 64 kDa was higher, while the expression of TSG101 protein at 43 kDa and CD9 protein at 26 kDa was lower. Third, differences in the expression of exosome surface proteins (E); the difference of cell exosomes in same surface protein (F).

Table 1. Characteristic protein markers of exosomes, assessed by immunoblot

Protein	MW (kDa)	Cell types secreting indicated exosomes protein	Enrichment
CD9	25	DC, IEC, U, P	High
CD63	50-60	Human: DC, B, IEC	High
TSG101	44	DC, Mov, U	High

DC: dendritic cells; IEC: intestinal epithelial cells; Mov: immortalized Schwann cells; U: urine; P: platelets

BCA protein concentration measurements of exosomes

Protein extraction: Sample buffer was added to each sample on ice, and the mixture was incubated for 20 minutes and then centrifuged at 6000 rpm for 5 minutes. The supernatant was collected for use.

Protein concentration measurements

BCA protein concentration detection method is used to detect the protein concentrations. Briefly, two hundred milligrams of albumin from bovine serum (BSA) was weighed and dissolved in 100 ml of NaCl at 150 mmol/l, creating a standard protein solution with a concentration of 2 mg/ml. Reaction solution A and reaction solution B were uniformly mixed at a ratio of 1:50 to create the working solution. The same amount of standard protein solution or test sample was added to 200 μl of working solution. The absorbance at 570 nm was determined for each sample, and a standard curve was drawn to figure out the concentration.

Protein analysis of exosomes

Measurement of exosomes protein concentrations: BCA protein concentration detection method is used to detect exosome protein concentrations (see details above).

Determine exosomes surface-specific molecular marker: These are some essential methods and procedure from Western blot test.

Raman spectra analysis

Exosome samples were diluted to different concentrations with filtered PBS. The exosomes (50 μl, 10^7 particles/ml) from colon cancer cells (Mc38 and CT26) and normal immune cells (Ala-1 cells from mouse) were placed on quartz glass grooves. The spectra were recorded within the 400-2000 cm^{-1} range with an acquisition time of 120 seconds per spectrum. The laser power of Raman experiment setup [20] was 15 mW, using a 532 nm solid state diode laser, and a 100× objective (Nikon, TE-2000). The type and content of exosome components (such as RNA, DNA, protein, fat and so on) were determined by the baseline and amplitude of the characteristic Raman spectrum.

Results

TEM Images

Figure 3 shows TEM images of a colon cancer cell-derived exosome and an immune cell-derived exosome. TEM indicated that the average exosome size was approximately 120 nm.

FCM

Figure 4 shows that CD63 and CD9 were stained with fluorescent antibodies in every exosome solution isolated by ultracentrifugation. Each kind of exosome particle was labeled with both fluorescein FITC and APC. Because the forward scatter (FSC) reflects the size of the particle and the side scatter (SSC) reflects the internal structure of the particle, the cross-border or tail phenomenon of some scatter plots may be related to the low purity of the exosome particles.

NTA

The NTA curves of the exosomes derived from two cell lines with differing degrees of malignancy (CT26, Mc38) and benign cells (Ala-1) were linear and smooth, indicating that there were few impurities, and the peaks of the particle size curves were 115.5 nm, 165.5 nm and 147.5 nm, respectively (**Figure 5A-C**). It was confirmed that most of the extracts had a particle size distribution of 30-200 nm.

BCA protein concentration detection

The BCA of culture supernatant exosomes from malignant cell lines (CT26 and Mc38) is much higher than that of benign cell lines (Ala-1). Similarly, analysis of three surface proteins on

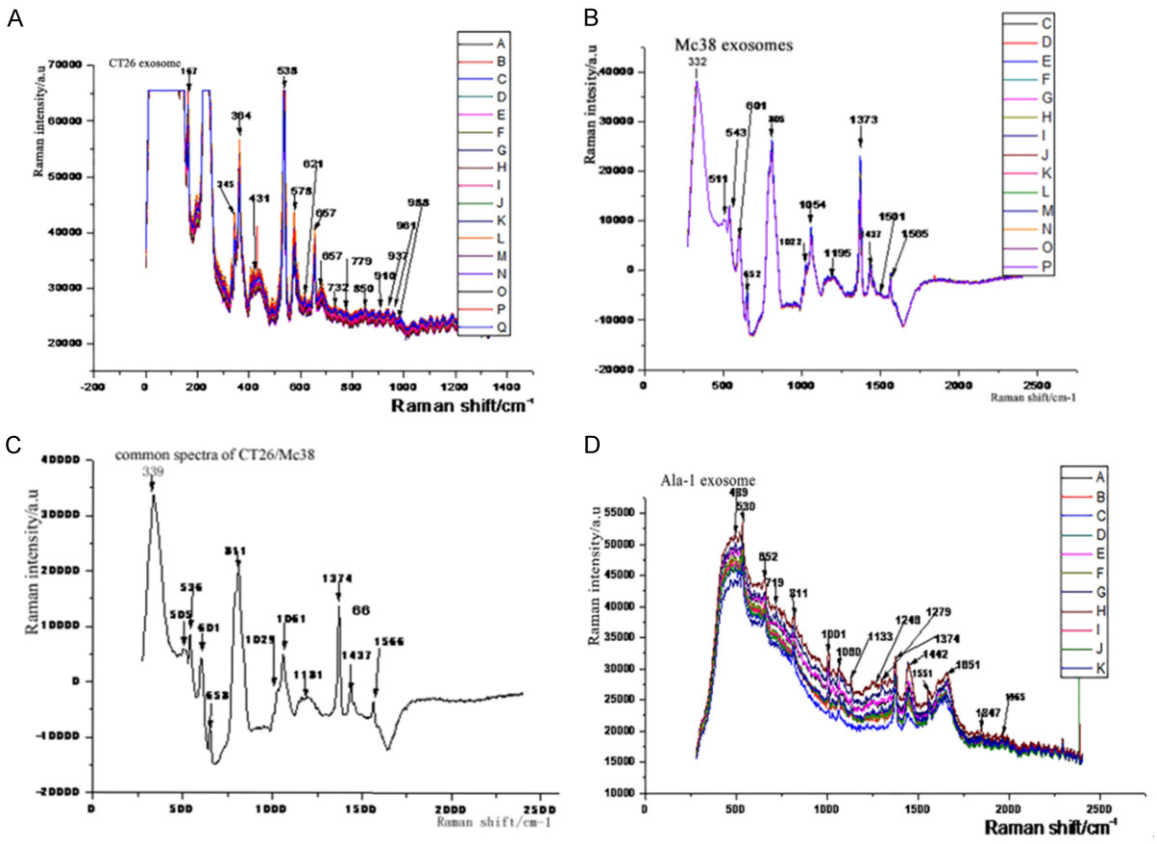

Figure 6. Raman spectra generated by the sample directly from the machine were used to analyze the position and intensity of each peak. The Raman position value of the peak is marked to help analyze and decode these data. (A, B, D) show that various substances in the exosomes of Mc38, CT26 and Ala-1 produce a variety of different characteristic spectra in the Raman spectrometer. The common spectra of malignant CT26 and Mc38 exosome (C) is different from that of benign Ala-1 exosome (D) in crucial spectra.

the same cells revealed that CD63 had the highest surface-specific protein concentration, followed by CD9, and TSG101 had the lowest.

Exosome marker proteins: WB was used to detect exosome-specific marker proteins (**Table 1**). **Figures 5D** and **7** clearly show that the bands corresponding to CD63 are clear and relatively wide at 66 kDa, indicating that the surface proteins are rich and high expression.

Through further analysis of the experimental data (**Table 2**), the expression levels of different exosome surface proteins were found to be different (**Figure 5E**), which means that the protein expression of malignant tumor cells is basically higher than that of normal benign cells. These also confirm that the expression of proteins and nucleic acids increased significantly after malignant transformation of cells. In addition, the same surface protein expression in different cell exosomes was also different from our group (**Figure 5F**), which means that the expression of surface proteins in malignant cells is substantially higher than that of normal benign cells.

Raman spectra

Origin 8.0 software was used to generate the spectra of four kinds of exosomes; **Figure 6** shows that the peak of the exosomes from the more malignant tumor cells was much higher. Therefore, the intensity of the Raman spectrum was higher than that of the low-malignancy Mc38 exosomes cells, which in turn was higher than that of the benign Ala-1 exosomes cells. In other words, intensity arrangement of Raman signal ($I_{CT26exo}$>$I_{Mc38exo}$>$I_{Ala\text{-}1exo}$) indicating that a higher degree of malignancy is associated with higher proportion of protein and nucleic acid content.

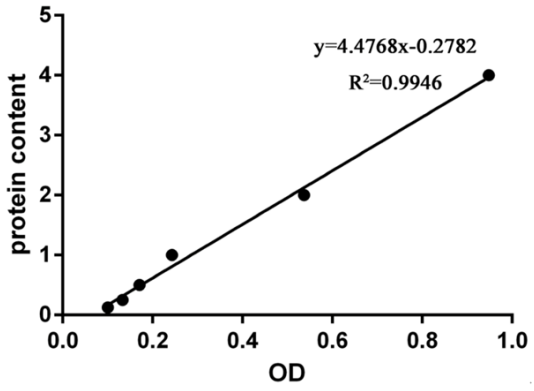

Figure 7. The relationship between OD value and protein content in curve equation.

According to two left column of each table (**Table 3-5**) from the Professional book [21, 22], there are many similar peaks in exosomes of colorectal cancer, which means that they contain many common substances and abundances, especially proteins and nucleic acids. The extrinsic performance spectra of these common substances will be a simple, non-invasive detection marker.

The following content will show these hidden common substances and mechanisms of action. These characteristic spectra weregenerated by fitting the spectra of CT26 exosomes and Mc38 exosomes together via observation and analysis of a third image. In the protein spectrum of CT26 exosomes, 960 cm^{-1} represents C-C, which is associated with the protein secondary structure random coil; 1225 cm^{-1} represents C-N str, N-Hdef (amide III); 621 cm^{-1} represents O=C-Ndef (amide IV); 657 cm^{-1}, 732 cm^{-1}, and 779 cm^{-1} represent N-Hdef (amide V); 538 cm^{-1} and 578 cm^{-1} represent C=Odef (amide VI); 333 cm^{-1}, 345 cm^{-1}, and 364 cm^{-1} represent nucleic acids; 431 cm^{-1} and 621 cm^{-1} represent base and carbohydrate deformation; and 779 cm^{-1} represents base, phosphodiester (OPO). The Raman shifts that correspond to Mc38exo include 952 cm^{-1}, 1215 cm^{-1}, 652 cm^{-1}, 652 cm^{-1}, 805 cm^{-1}, 543 cm^{-1}, 601 cm^{-1}, 332 cm^{-1}, 511 cm^{-1}, 543 cm^{-1}, 601 cm^{-1}, 652 cm^{-1}, and 805 cm^{-1}. These corresponding spectra associated with representative substances show that there are many common features and characteristics of cancer cells in the fitted average spectrum.

In this fitted average spectrum, the spectra of proteins, nucleic acids, and even lipids appear simultaneously. For example, the corresponding protein spectrum containing 658 cm^{-1}, 803 cm^{-1} N-Hdef (amide V), 536 cm^{-1}, and 601 cm^{-1} also represents C=Odef (amide VI), and the corresponding nucleic acid spectrum peaks are 339 cm^{-1} and 505 cm^{-1}. The 536 cm^{-1} and 601 cm^{-1} peaks represent base, carbohydrate deformation, and 658 cm^{-1} represents base, phosphodiester (OPO). Therefore, with this spectrally fitted spectrum, an exosome spectrum of cells that differ in type and malignancy was observed. When we compared the intensity of the peaks, the average intensity of the observed spectrum was lower than that of the original spectrum. Therefore, from this fitted average characteristic spectrum that Raman spectra with these characteristic peaks in the biological spectrum are cancerous spectra, representing the standard spectrum of malignancy. The biological spectrum containing these characteristics reveals that cells may have undergone cancerous transformation.

Table 2. Area (grayscale value) under the curve from exosome-specific protein

		Sample		
		CT26	Mc38	Ala-1
Primary	CD9	1355	346	262
	CD63	27997	3447	14009
	TSG101	438	319	110

Discussion

According to Siegel, et al. [23], although the annual mortality rates of cancer have slightly declined in the United States, the overall situation remains pessimistic. If it is diagnosed early, the cure rate could be more than 90%. With the rapid development of optics, Raman spectra, and in particular laser optical tweezers with Raman spectra, possesses many advantages for diagnosis via exosomes.

In this study, two kinds of CRC cells with different degrees of malignancy and Ala-1 macrophages were studied. Supernatants from the cultured cells were collected and then ultracentrifuged to obtain exosomes. A series of exosome identification methods, such as TEM, FCM, NTA, and WB, were employed.

Through the analysis of the experimental data, we conclude the following results:

Table 3. Raman frequencies and peak assignments of amide acids

Raman Frequencies of Amide Acids and peak assignments		CT26 exosomes	Mc38 exosomes	Tumor average spectra	Ala-1 exosomes
890-945	C-C (α-helix Protein secondary structure)	886,910,937			
945-960	C-C (random coil Protein secondary structure)	960	952		
1597-1680	C=Ostr N-Hdef C-Nstr amide I				1651
1480-1575	C-Nstr N-Hdef amide II		1565	1480, 1566	1551
1229-1305	C-Nstr N-Hdef amide III	1225	1215		1279
625-767	O=C-Ndef amide IV	621	652		760
640-800	N-Hdef amide V	657,732,779	652,805	658,803	
537-606	C=Odef amide VI	538,578	543,601	536,601	536
200	C-Nstrtor amide VII	198			

Table 4. Raman frequencies and peak assignments of nucleic acids

Raman Frequencies of Nucleic Acids and peak assignments		CT26 exosomes	Mc38 exosomes	Average spectra	Ala-1 exosomes
300-650	base carbohydrate deformation	333,345,364 431,621	332,511,543 601,652	339,505 536,601	489,536
650-800	Base phosphodiester (O-P-O)	779	805	658	652,719,760
1250-1450	base		1437	803,1237,1374	1246, 1279
1300-1460	Base carbohydrate def (C-H)		1373	1437	1374, 1442
1450-1550	base str		1501	1480	
1550-1650	Base (C=H, C=C)			1566	
1600-1750	Base (C=Ostr NHdef)				

Table 5. Raman frequencies and peak assignments of lipid

		CT26 exosomes	Mc38 exosomes	Average spectrum	Ala-1
1066	Phosphatidyl c-c spectrum anti-form		1054	1061	Exosomes
1130	Phosphatidyl c-c spectrum anti-form	1135			
1090	Phosphatidyl c-c spectrum tor				

First, the protein expression of malignant tumor cells is basically higher than that of normal benign cells. From the expression level of CD63, CD9, TSH101 protein in normal and tumor cell, the expression of tumor cell exosomes are higher than those of normal benign cell exosomes, which is related to the high metabolism of malignant cells. Highly metabolized malignant cells express more proteins such as membrane proteins and embryonic proteins, so exosomes produced by shedding also contain more proteins. A new related test has been carried out that the surface protein profiles of two live cancer cell lines are compared with an antibody microarray and Biotinylated antibodies. These EV expressed from the same patients: moderate or high levels of CD5, CD19, CD31, CD44, CD55, CD82; low levels of CD21, CD63. But none of these proteins could not be detected on EV from matched healthy individuals. This also confirms that some exosome surface proteins are highly expressed in tumor cell extracellular bodies, and are low or not expressed in normal cells, which is consistent with the results of this experiment [24].

Second, the same surface protein expression in normal and tumor cell exosomes is also different, which suggests that the expression of surface proteins in malignant cells is significantly higher than that of normal benign cells. Finally, there are many similar peaks in exosomes of colorectal cancer after analyzing a large number of different Raman spectras, which means that they contain many common

substances and abundances in crucial proteins and nucleic acids.

There are some limitations to our study. First, large numbers of cancer cell exosomes derived from different disease types and perform Raman spectroscopy are needed. Second, to analyze and compare all these cell types in aggregate is needed. Future efforts will be devoted to exploring this hidden standard for cancer diagnosis.

In summary, this novel method is non-invasive and can be used in clinical diagnosis to observe tiny biomolecular structures in situ which is suitable for biomarker discovery studies.

Acknowledgements

The authors thank Pro. Zhang Sen for expert technical and academic assistance, Dr. Chen Jianxin and Dr. Xu Xiong for assistance in ultracentrifugation and Dr. Huang Wei, Dr. Zhou Jiqiu for assistance in NTA measurements and WB. Dr. Xu Gang for assistance in FCM.

Acknowledgements

This study was supported by the National Natural Science Foundation of China (No: 30672059).

Disclosure of conflict of interest

None.

Address correspondence to: Sen Zhang, Department of Colorectal Surgery, The First Affiliated Hospital of Guangxi Medical University, 22 Shuangyong Road, Nanning, Guangxi 530021, P.R. China. Tel: +86-18738505902, E-mail: zhangsen5434664@163.com

References

[1] Siegel RL, Miller KD, Fedewa SA, Ahnen DJ, Meester RGS, Barzi A and Jemal A. Colorectal cancer statistics, 2017. CA Cancer J Clin 2017; 67: 177-193.

[2] Pardal R, Clarke MF and Morrison SJ. Applying the principles of stem-cell biology to cancer. Nat Rev Cancer 2003; 3: 895.

[3] Hannafon BN, Carpenter KJ, Berry WL, Janknecht R, Dooley WC and Ding WQ. Exosome-mediated microRNA signaling from breast cancer cells is altered by the anti-angiogenesis agent docosahexaenoic acid (DHA). Mol Cancer 2015; 14: 133.

[4] Thery C, Zitvogel L and Amigorena S. Exosomes: composition, biogenesis and function. Nat Rev Immunol 2002; 2: 569-579.

[5] Grange C, Tapparo M, Collino F, Vitillo L, Damasco C, Deregibus MC, Tetta C, Bussolati B and Camussi G. Microvesicles released from human renal cancer stem cells stimulate angiogenesis and formation of lung premetastatic niche. Cancer Res 2011; 71: 5346-5356.

[6] Caradec J, Kharmate G, Hosseini-Beheshti E, Adomat H, Gleave M and Guns E. Reproducibility and efficiency of serum-derived exosome extraction methods. Clinical biochemistry 2014; 47: 1286-1292.

[7] Mincheva-Nilsson L, Baranov V, Nagaeva O and Dehlin E. Isolation and characterization of exosomes from cultures of tissue explants and cell lines. Curr Protoc Immunol 2016; 115: 14.42.1-14.42.21

[8] Rekker K, Saare M, Roost AM, Kubo AL, Zarovni N, Chiesi A, Salumets A and Peters M. Comparison of serum exosome isolation methods for microRNA profiling. Clin Biochem 2014; 47: 135-138.

[9] Shao H, Im H, Castro CM, Breakefield X, Weissleder R and Lee H. New technologies for analysis of extracellular vesicles. Chem Rev 2018; 118: 1917-1950.

[10] Borel S, Prikryl EA, Vuong NH, Jonkman J, Vanderhyden B, Wilson BC and Murugkar S. Discrimination of normal and malignant mouse ovarian surface epithelial cells in vitro using Raman microspectroscopy. Anal Meth 2015; 7: 9520-9528.

[11] van der Pol E, Hoekstra AG, Sturk A, Otto C, van Leeuwen TG and Nieuwland R. Optical and non-optical methods for detection and characterization of microparticles and exosomes. J Thromb Haemost 2010; 8: 2596-2607.

[12] Tatischeff I, Larquet E, Falcon-Perez JM, Turpin PY and Kruglik SG. Fast characterisation of cell-derived extracellular vesicles by nanoparticles tracking analysis, cryo-electron microscopy, and Raman tweezers microspectroscopy. J Extracell Vesicles 2012; 1.

[13] Ito H, Tanimura Y. Simulating two-dimensional infrared-Raman and Raman spectroscopies for intermolecular and intramolecular modes of liquid water. J Chem Phys 2016; 144: 074201.

[14] Yeung A, Dabros T, Masliyah J and Czarnecki J. Micropipette: a new technique in emulsion research. Colloids and Surfaces A: Physicochemical and Engineering Aspects 2000; 174: 169-181.

[15] Wang H, Zhuang XH, Hillmer S, Robinson DG and Jiang LW. Vacuolar sorting receptor (VSR)

proteins reach the plasma membrane in germinating pollen tubes. Molecular Plant 2011; 4: 845-853.
[16] Carney RP, Hazari S, Colquhoun M, Tran D, Hwang B, Mulligan MS, Bryers JD, Girda E, Leiserowitz GS, Smith ZJ and Lam KS. Multispectral optical tweezers for biochemical fingerprinting of CD9-positive exosome subpopulations. Anal Chem 2017; 89: 5357-5363.
[17] Eckmann A, Felten A, Mishchenko A, Britnell L, Krupke R, Novoselov KS and Casiraghi C. Probing the nature of defects in graphene by Raman spectroscopy. Nano letters 2012; 12: 3925-3930.
[18] Lee CW and Tseng FG. Surface enhanced Raman scattering (SERS) based biomicrofluidics systems for trace protein analysis. Biomicrofluidics 2018; 12: 011502.
[19] van Niel G, D'Angelo G and Raposo G. Shedding light on the cell biology of extracellular vesicles. Nat Rev Mol Cell Biol 2018; 19: 213-228.
[20] Lin M, Xu B, Yao H, Shen A and Hu J. An in vivo quantitative Raman-pH sensor of arterial blood based on laser trapping of erythrocytes. Analyst 2016; 141: 3027-3032.
[21] Yiming X. Protein Raman spectra. Raman Spectroscopy and Its Application in Structural Biology 2005; 1: 11-31.
[22] Yiming X. Raman spectra of nucleic acids. Raman Spectroscopy and Its Application in Structural Biology 2005; 36-58.
[23] Siegel RL, Miller KD and Jemal A. Cancer statistics, 2017. CA Cancer J Clin 2017; 67: 7-30.
[24] Belov L, Matic KJ, Hallal S, Best OG, Mulligan SP and Christopherson RI. Extensive surface protein profiles of extracellular vesicles from cancer cells may provide diagnostic signatures from blood samples. J Extracell Vesicles 2016; 5: 25355.